18TH INTERNATIONAL CONGRESS ON SOUND & VIBRATION
ICSV18
RIO DE JANEIRO
BRAZIL
10–14 JULY 2011

NOISE REDUCTION IN DOUBLE-PANEL STRUCTURES BY CAVITY AND PANEL RESONANCE CONTROL

Jen-Hsuan Ho

Department of Electrical Engineering, University of Twente, Drienerlolaan 5, P.O.Box 217 7500 AE Enschede, The Netherlands
e-mail: j.ho@utwente.nl

Arthur Berkhoff

TNO, Acoustics Department, P.O. Box 155, 2600AD Delft, The Netherlands
e-mail: arthur.berkhoff@tno.nl
Department of Electrical Engineering, University of Twente, Drienerlolaan 5, P.O.Box 217 7500 AE Enschede, The Netherlands
e-mail: a.p.berkhoff@utwente.nl

This paper presents an investigation of the cavity and the panel resonance control in a double-panel structure. The double-panel structure, which consists of two panels with air in the gap, is widely adopted in many applications such as aerospace due to its light weight and effective transmission-loss at high frequency. However, the resonance of the cavity and the poor transmission-loss at low frequency limit its noise control performance. Applying active control forces on the panels or utilizing loudspeakers in the cavity to reduce the noise problem have been discussed in many papers. In this paper, the resonance of the cavity and the panels are considered simultaneously to increase the noise transmission-loss. A structural-acoustic coupled model is developed to investigate the vibration of the two panels, the acoustic resonance in the air cavity, and the control performance. The control design can be optimized through the model. Finally, the results will be presented and discussed.

1. Introduction

Noise control technology is an important issue with the increasing importance of a comfortable environment. Adding damping materials and installing resonators in the system can effectively reduce the noise at high frequencies[1, 2]. However, passive control at low frequencies usually has much less noise reduction and comes with a heavy implementation because the acoustic wavelengths are much longer than the damping structure[3, 4]. On the other hand, with the advance of smart materials and computational power, active noise control has received increasing attention in the last decades due to the possible advantages of reduced weight and better performance at low frequencies. Active noise control (ANC) has been applied successfully in relatively small regions of space in case of broadband noise control[5-7]. However, the acoustic wave is a 3D propagation problem; for a larger noise control region, the implementation will become very complicated and inefficient. Acoustic structural active control (ASAC) can simplify 3D acoustic wave problem to 2D structural vibration problem by directly applying actuators on the structure to reduce the radiation sound pressure from the structure[6, 8]. Furthermore, for a large configuration, decentralized control or distributed control can bring the controller to more practical implementations[9-13]. Control methods also need to consider the additional weight of the installation[14], double panel with an air gap structure is another common method to reduce sound transmission since it has a lightweight structure[1, 15]. Due to the compact dimensions and the fast response, piezoelectric materials have been investigated and applied frequently for vibration control of smart structures[5, 12, 16]. It has been noted that the decentralized feedback control strategy performs remarkably well for the broadband objective[17].

In this paper, the resonant behavior of the double panel structure is analyzed. The structural control and the cavity control with feedback control were simulated to derive the optimized control effect. This paper is composed of four sections. First, the multiple fully coupled interaction control theory and the stability analysis method are introduced. Second, the finite element method model and the experiment measurement methods are described. Then, the multiple feedback control results of the structure control, the cavity control and the combination control are shown and discussed.

2. Multiple decentralized control

For a feedback control system, the signal block diagram is illustrated in Fig. 1. $\mathbf{G}(j\omega)$ is the plant response matrix, $\mathbf{H}(j\omega)$ is the controller matrix, $\mathbf{y}(j\omega)$ is the error signal matrix detected by the sensors, and $\mathbf{d}(j\omega)$ is the noise source signal matrix which is the error signal without input control signals.

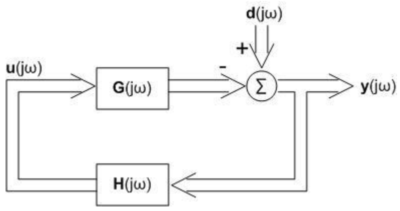

Figure 1. Direct velocity feedback systems.

From the block diagram above, $\mathbf{y}(j\omega)$ can be represented as Eq. (1)

$$\begin{aligned}\mathbf{y}(j\omega) &= \mathbf{d}(j\omega) - \mathbf{y}(j\omega)\cdot\mathbf{G}(j\omega)\mathbf{H}(j\omega)\\ \mathbf{y}(j\omega) &= (\mathbf{I}+\mathbf{G}(j\omega)\mathbf{H}(j\omega))^{-1}\cdot\mathbf{d}(j\omega)\end{aligned} \tag{1}$$

In order to present the realistic physical property of the control system, the interactions between each control unit need to be considered. $\mathbf{G}(j\omega)$ in Eq. (1) is a multiple channel plant transfer matrix,

$$\mathbf{G}(j\omega) = \begin{bmatrix} \mathbf{G}_{11}(j\omega) & \cdots & \mathbf{G}_{1m}(j\omega) \\ \vdots & \ddots & \vdots \\ \mathbf{G}_{l1}(j\omega) & \cdots & \mathbf{G}_{lm}(j\omega) \end{bmatrix} \tag{2}$$

where $\mathbf{G}_{lm}(j\omega)$ is the response at the l^{th} sensor under the input from m^{th} actuator without the disturbance source $\mathbf{d}(j\omega)$.

The stability of a feedback control system can be unconditionally guaranteed when the sensors and the actuators are dual and collocated. Otherwise, the control gain will be limited. To determine the stability of MIMO decentralized control systems, the Nyquist criterion can be used. When the plot of Eq. (3) does not cross nor encircle the origin (0, 0), the system is stable[17].

$$\det[\mathbf{I}+\mathbf{G}(j\omega)\mathbf{H}(j\omega)] \tag{3}$$

3. Model analysis and measurement

3.1 Acoustic-structural interaction FEM model

The numerical analysis is based on the finite element method (FEM) using Comsol. To estimate the characteristics of the system, the acoustic and structural properties need to be considered simultaneously. The relationship of the acoustic pressure in the fluid domain and the structural deformation in the solid domain are linked as described below. In the solid domain, the fluid pressure p produces a normal force $\mathbf{F}_p$ on the fluid-solid interacting boundaries,

$$\mathbf{F}_p = -\mathbf{n}_s p \tag{4}$$

In which $\mathbf{n}_s$ is the normal vector of the solid boundaries. In the acoustic fluid domain, the acceleration $\mathbf{u}_{tt}$ of the structure is identical to the acceleration of the fluid-solid interacting boundaries,

$$a_n = \mathbf{n} \cdot \mathbf{u}_{tt} \tag{5}$$

With Eq. (4) and Eq. (5), the interaction between the acoustic field and the solid structure can be investigated.

To analyze the resonant behavior and the sound transmission of a double panel, the model is assumed to contain two simply supported panels and a cavity with 35mm thickness. The primary noise source is presented as an incident spherical pressure wave from the corner of the bottom side in order to simulate an asymmetric incident noise wave (Fig. 2). The parameters used for the simulation model are given in Table 1. The acrylic box is modeled with a hard-wall boundary.

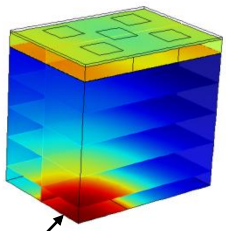

Figure 2. Acoustic-strucutre interaction model.

Table 1. Model parameters

	Parameters	Values	unit
Aluminum panel	Dimensions	420*297*1	[mm^3]
	Density	2700	[kg/m^3]
	Young's modulus	70	[GPa]
	Poisson's ratio	0.33	
	Loss factor	0.03	
Honeycomb panel	Dimensions	420*297*5.8	[mm^3]
	Density	409	[kg/m^3]
	Young's modulus	3.7	[GPa]
	Poisson's ratio	0.33	
	Loss factor	0.03	
PZT patches	Dimensions	7.24*7.24*0.264	[mm^3]
	Density	7800	[kg/m^3]
	Young's modulus	52	[GPa]
	Poisson's ratio	0.33	
	Strain coefficient d_{31}	-190	[meter/Volt]
Acrylic box	Inner Dimensions	420*297*350	[mm^3]
	Wall thickness	40	[mm]
Middle cavity	Inner Dimensions	420*297*35	[mm^3]

3.2 Piezoelectric actuators

Piezoelectric materials have the advantages of fast response and compact dimensions. The effect of laminar piezoelectric patches attached to a plate can be represented as four line moments on the edges of the piezoelectric patch[18] (Fig. 3). E_p is the Young's modulus of the piezoelectric patch, V is the controlling voltage applied to the patch, d_{31} is the piezoelectric constant, M_p is the moment per unit length. The piezoelectric control force is presented as these four line moments in our numerical analysis.

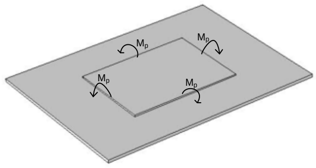

Figure 3. Equivalent piezoelectric loads.

$$M_p = -E_p d_{31} h V \quad (6)$$

3.3 Double panel with acrylic box

To prove the control effect, a double panel mounted on a rectangular box was set up for measurement. The primary noise source is generated by a loudspeaker in the bottom of the rectangular box. This box is made with 40 mm thickness of walls of acrylic plates to prevent the sound from leaking through side walls. The inner dimensions of the box are 420*297*350 mm^3. The primary noise source first entered an aluminum panel (the incident panel), then a layer of air of 35mm thickness followed by a honeycomb panel (the radiating panel). The transmitted sound of this double panel structure can be measured above the radiating panel (Fig. 4).

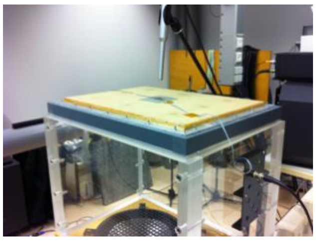

Figure 4. Experiment setup and measurement.

4. Simulation and experiment results

In the numerical analysis, structural control, cavity control, and combined control will be compared.

4.1 Model validation

To validate the numerical analysis, the comparison of the kinetic energy response of a single panel for excitation with one piezoelectric patch is shown in Fig. 5. The kinetic energy of the panel was measured by nine accelerometers on the surface. To further validate the structural-acoustic interaction result, a double panel model and the experimental measurement are compared. In Fig. 6, the number of the resonant peaks increases because of the resonance contributions from the incident panel and the cavity. Fig. 5 shows that the numerical model can accurately present the practical sensor-actuator response in a single panel structure. Fig. 6 shows that the numerical model can present the practical sensor-actuator response in a double panel structure with reasonable accuracy.

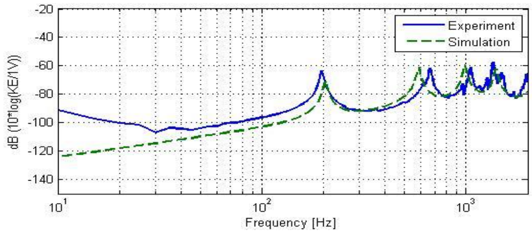

Figure 5. Kinetic energy of the single panel.

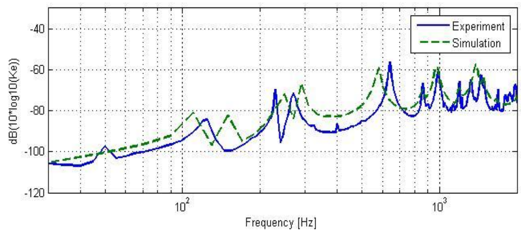

Figure 6. Kinetic energy of radiating panel in double panel structure.

4.2 Structural control

Regarding structural control, pzt actuators are expected to have excellent control performance on smart structures and also are applied in active noise control. Therefore piezoelectric patches are installed on the radiating honeycomb panel with velocity sensors located in collocated positions to control the vibration of the panel.

4.2.1 Numerical analysis

The configuration of five control sets is shown in Fig. 7. To ensure the stability of the structure control loop, the maximum control gain can be found by utilizing Nyquist analysis. Fig. 8 shows the response of a control gain of 500. The plot does not encircle the origin which guarantees stability of the system for a control gain of 500.

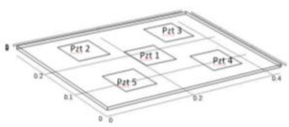

Figure 7. Control sets on the radiating panel.

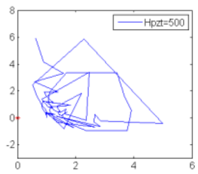

Figure 8. Nyquist plot from 10-1000Hz.

Nevertheless, the reduction of double panel resonance with the pzt actuator located on the radiating panel is limited at the resonance frequencies 80Hz, 140Hz, 190Hz. On the other hand, the peaks at 330Hz, 400Hz, 520Hz, 720Hz have noticeable reductions (Fig. 9). The resonant mode shapes of the double panel structure are shown in Table 2. Compared to the reduction response plot, it can be seen that when the resonance is not dominated by the radiating panel, the pzt actuators hardly lead to the noise reduction.

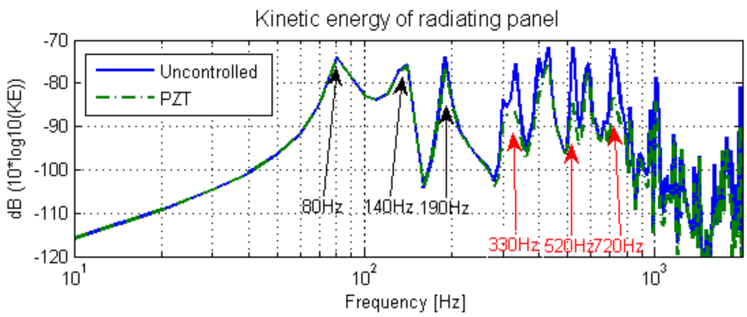

Figure 9. Kinetic energy of the radiating panel.

Table 2. Mode shapes of the incident panel (bottom panel) and the radiating panel (top panel).

	80	140	190	330	400
Uncontrolled	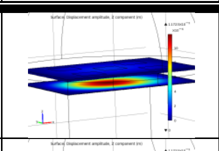	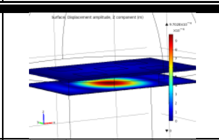	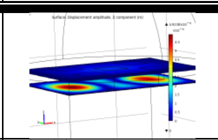	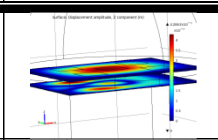	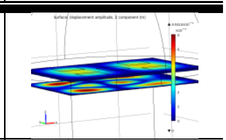
5pzt h500	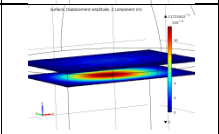	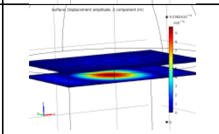	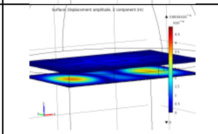	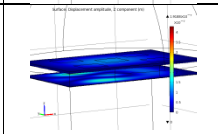	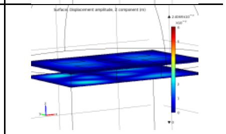

	430	520	590	720	820
Uncontrolled	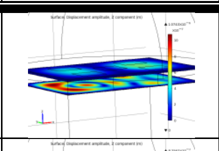	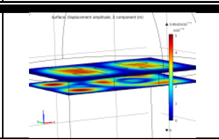	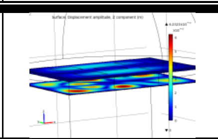	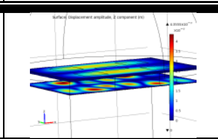	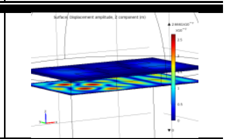
5pzt h500	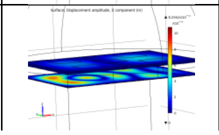	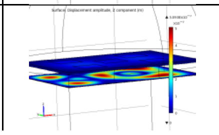	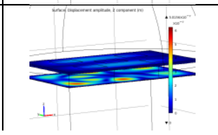	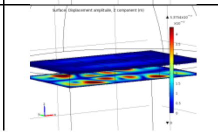	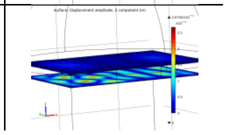

4.2.2 Real time feedback control experiment result

To compare the control effect of pzt actuators on a single panel structure and a double panel structure, a single pzt actuator and a velocity sensor were installed on the centre of the radiating panel surface. The difference between these two measurements is, in the single panel structure, the radiating panel directly receives the incident noise whereas in the double panel structure, the noise source first passes through an incident panel and a cavity. The experimental result in Fig. 10 and Fig. 11 shows that pzt actuators on the radiating panel only ensure a significant influence on the vibration level of the single panel structure. Since only a single central pzt patch is used, only the mode with lowest resonance frequency can be controlled. In the double panel structure, almost no reduction of the vibration level can be noticed.

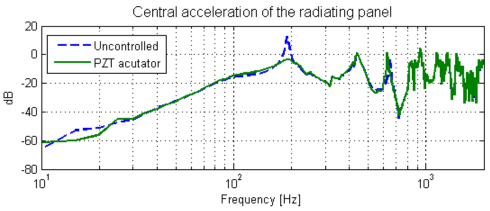

Figure 10. Single panel structure.

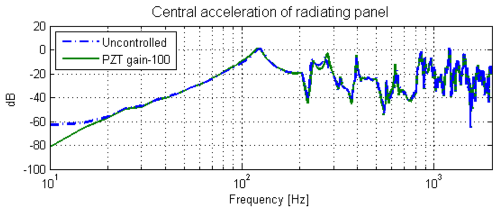

Figure 11. Double panel structure.

4.3 Cavity control

In the double panel structure, the resonance from the cavity dominates considerably resonant energy as well. To reduce the resonance in the cavity, six decentralized controller were installed in the middle cavity between these double panels. Each controller detects sound pressure with one microphone and produces a secondary pressure source by one loudspeaker from the side of the cavity. The distribution of these six control sets is shown in Fig12.

The influence from the actuators to each sensor is considered simultaneously to derive the total plant transfer function $\mathbf{G}(j\omega)$. From the Nyquist plot of $\det[\mathbf{I}+\mathbf{G}(j\omega)\mathbf{H}(j\omega)]$ in Fig. 13, the response does not pass through the origin. It shows the system is stable with constant feedback control gain 0.06.

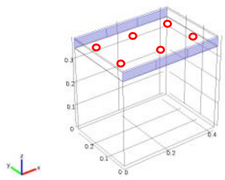

Figure 12. Control sets distribution.

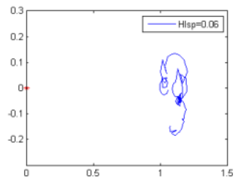

Figure 13. Nyquist plot from 10-1000Hz.

In a realistic control system, loudspeakers can be assumed to operate as acceleration sources above the resonance frequency instead of a pressure sources. The cavity feedback control system in practical applications can be assumed to perform as stable as the model with pressure control source in the previous section, as can be seen from the bode plot for an acceleration source and a pressure sensor (Fig. 14).

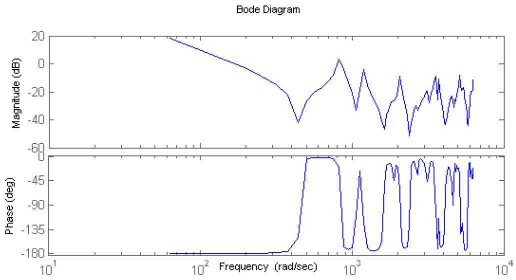

Figure 14. Bode plot of the acceleration control source**.**

4.4 Combined control

The stability of cavity control (loudspeaker and microphone combinations) and structural control (piezoelectric actuators and velocity sensors) can be analyzed with the fully coupled plant transfer function where the 11 actuators and 11 sensors are considered simultaneously. Fig. 16 shows the Nyquist plot of the stability analysis. The frequency responses of the control effect by different control strategies are shown in Fig. 17. It shows that the combination can further improve the control effect when the structural control of the radiating panel is limited due to the incident panel and the cavity dominated resonant modes.

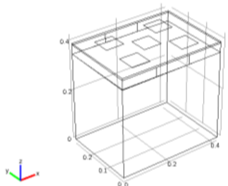

Figure 15. Combination model.

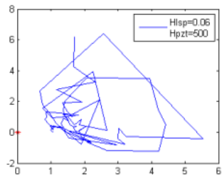

Figure 16. Combined stability analysis.

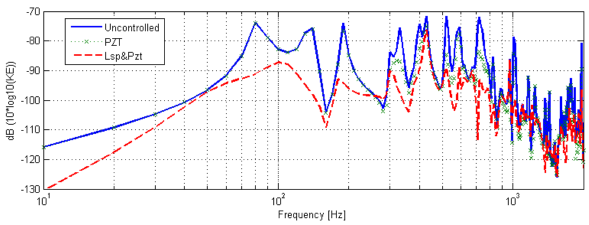

Figure 17. Comparison of different control methods.

5. Conclusions

This paper has shown that although pzt actuators can effectively reduce the noise from a single panel structure, it can only have better performance when the noise is dominated by the resonance of the radiating panel in a double simply supported panel structure. To further improve the control effect, a combination with cavity control can improve the performance.

Based on the resonant behavior of the double panel structure, as an alternative to cavity control, pzt actuators should not be applied only on the radiating panel, the incident panel should be considered simultaneously. Use of pzt actuators both on the radiating panels and the incident panels, or use of actuators which have a stronger link between these two panels are expected to lead to better control performance.

6. Acknowlegements

The research and development is funded by STW, project IMPEDANCE (Integrated Modules for Power Efficient Distributed Active Noise Cancelling Electronics). The experimental development has been supported by Henny Kuipers and Geert Jan Laanstra of Signals and Systems group, Faculty of EEMCS, University of Twente.

REFERENCES

1. M. Qibo and S. Pietrzko, "Experimental study for control of sound transmission through double glazed window using optimally tuned Helmholtz resonators," *Applied Acoustics*, 71, pp. 32-8 (2010).
2. C. Hirunyapruk, *et al.*, "A tunable magneto-rheological fluid-filled beam-like vibration absorber," *Smart Materials and Structures*, **19**, p. 055020 (10 pp.) (2010).
3. F. Fahy and J. Walker, *Fundamentals of Noise and Vibration*, Routledge, UK, (1998).
4. F. Fahy and P. Gardonio, *Sound and structural vibration: radiation, transmission and response* 2ed Edition, Academic Press, Elsevier, London (2007).
5. O.E. Kaiser, S.J. Pietrzko,M.Morari, "Feedback control of sound transmission through a double glazed window", *Journal of Sound and Vibration* **263** 775–795(2003).
6. J. Pan, C. Bao, "Analytical study of different approaches for active control of sound transmission through double walls", *Journal of the Acoustical Society of America* **103** (2) 1916–1922 (1998).
7. S. Pietrzko, O. Kaiser, "Experiments on active control of air-borne sound transmission through a double wall cavity", *Proceeding of International Symposium on Active Control of Sound and Vibration*, Florida, pp. 355–362, (1999).
8. J.P. Carneal, C.R. Fuller, "An analytical and experimental investigation of active structural acoustic control of noise transmission through double panel systems", *Journal of Sound and Vibration* **272** 749–771(2004).
9. P. Gardonio, *et al.*, "Smart panel with multiple decentralized units for the control of sound transmission. Part I: theoretical predictions," *Journal of Sound and Vibration* **274**, pp. 163-92 (2004).
10. P. Gardonio, *et al.*, "Smart panel with multiple decentralized units for the control of sound transmission. Part II: design of the decentralized control units," *Journal of Sound and Vibration*, **274**, pp. 193-213 (2004).
11. P. Gardonio, *et al.*, "Smart panel with multiple decentralized units for the control of sound transmission. Part III: control system implementation," *Journal of Sound and Vibration*, **274**, pp. 215-32, (2004).
12. A. P. Berkhoff and J. M. Wesselink, "Combined MIMO adaptive and decentralized controllers for broadband active noise and vibration control", *Proceeding of International Symposium on Active Control of Sound and Vibration*, Ottawa, Canada, pp. 1-12 (2009).
13. P. A. Nelson and S. J. Elliott, *Active Control of Sound*, 1st Edition, Academic Press, London: (1992).
14. A. P. Berkhoff, "Weight reduction and transmission loss tradeoffs for active/passive panels with miniaturized electronics," *Proceeding of International Symposium on Active Control of Sound and Vibration*, Washington DC, USA, pp. 1-12 (2004).
15. N. Alujevic, *et al.*, "Smart double panel with decentralized active dampers for sound transmission control," *AIAA Journal*, **46**, pp. 1463-75 (2008).
16. A. P. Berkhoff, "Piezoelectric sensor configuration for active structural acoustic control," *Journal of Sound and Vibration*, **246**, pp. 175-83 (2001).
17. S. J. Elliott, *et al.*, "Active vibroacoustic control with multiple local feedback loops," *Journal of the Acoustical Society of America*, **111**, pp. 908-15 (2002).
18. A. Preumont, *Vibration control of active structures*, 2ed Edition, Kluwer Academic Publishers, New York (2004).